The interplay between autophagy and chloroplast vesiculation pathways under dark-induced senescence

Wagner Araújo[1], Jessica Barros[1], João Cavalcanti[2], Karla Pimentel[1], Sahar Magen[3], Yoram Soroka[3], David Barbosa Medeiros[4], Adriano Nunes-Nesi[1], Alisdair R. Fernie[4], and Tamar Avin-Wittenberg[3]

[1]Universidade Federal de Vicosa Departamento de Biologia Vegetal
[2]Universidade Federal do Amazonas
[3]Hebrew University of Jerusalem Department of Plant and Environmental Sciences
[4]Max-Planck-Institut fur molekulare Pflanzenphysiologie

March 3, 2023

Abstract

In cellular circumstances where carbohydrates are scarce, plants can use alternative substrates for cellular energetic maintenance. In plants, the main protein reserve is present in the chloroplast, which contains most of the total leaf proteins and represents a rich source of nitrogen and amino acids. Autophagy plays a key role in chloroplast breakdown, a well-recognized symptom of both natural and stress-induced plant senescence. Remarkably, an autophagic-independent route of chloroplast degradation associated with Chloroplast Vesiculation (CV) gene was recently demonstrated. During extended darkness, CV is highly induced in the absence of autophagy, contributing to the early senescence phenotype of *atg* mutants. To further investigate the role of CV under dark-induced senescence conditions, mutants with low expression of CV (*amircv*) and double mutants *amircv1xatg5* were characterized. Following darkness treatment, no aberrant phenotypes were observed in *amircv* single mutants; however, *amircv1xatg5* double mutants displayed early senescence and enhanced dismantling of chloroplast and membrane structures under these conditions. Metabolic characterization revealed that the functional lack of both CV and autophagy leads to higher impairment of amino acid release and differential organic acid accumulation during starvation conditions. The data obtained are discussed in the context of the role of CV and autophagy, both in terms of cellular metabolism and the regulation of chloroplast degradation.

Title :

The interplay between autophagy and chloroplast vesiculation pathways under dark-induced senescence

Authors:

Jessica A. S. Barros[a], João Henrique F. Cavalcanti[b], Karla G. Pimentel[a], Sahar Magen[c], Yoram Soroka[c], David B. Medeiros[d], Adriano Nunes-Nesi[a], Alisdair R. Fernie[d], Tamar Avin-Wittenberg[c] and Wagner L. Araújo[a]*

Affiliation:

[a] Departamento de Biologia Vegetal, Universidade Federal de Viçosa, 36570-900 Viçosa, Minas Gerais, Brazil

[b] Instituto de Educação, Agricultura e Ambiente, Universidade Federal do Amazonas, 69800-000, Humaitá, Amazonas, Brazil

[c] Department of Plant and Environmental Sciences, The Alexander Silberman Institute of Life Sciences, the Hebrew University of Jerusalem, Givat Ram, Jerusalem 9190401 Israel

[d] Max Planck Institute of Molecular Plant Physiology, Am Mühlenberg 1, D-14476 Potsdam-Golm, Germany

ABSTRACT

In cellular circumstances where carbohydrates are scarce, plants can use alternative substrates for cellular energetic maintenance. In plants, the main protein reserve is present in the chloroplast, which contains most of the total leaf proteins and represents a rich source of nitrogen and amino acids. Autophagy plays a key role in chloroplast breakdown, a well-recognized symptom of both natural and stress-induced plant senescence. Remarkably, an autophagic-independent route of chloroplast degradation associated with Chloroplast Vesiculation (CV) gene was recently demonstrated. During extended darkness, CV is highly induced in the absence of autophagy, contributing to the early senescence phenotype of *atg* mutants. To further investigate the role of CV under dark-induced senescence conditions, mutants with low expression of CV (*amircv*) and double mutants *amircv1xatg5* were characterized. Following darkness treatment, no aberrant phenotypes were observed in *amircv* single mutants; however, *amircv1xatg5*double mutants displayed early senescence and enhanced dismantling of chloroplast and membrane structures under these conditions. Metabolic characterization revealed that the functional lack of both CV and autophagy leads to higher impairment of amino acid release and differential organic acid accumulation during starvation conditions. The data obtained are discussed in the context of the role of CV and autophagy, both in terms of cellular metabolism and the regulation of chloroplast degradation.

Keywords: Autophagy, Carbon starvation, Chloroplast degradation, Senescence.

INTRODUCTION

Under environmental and developmental conditions that lead to carbohydrate limitation, plants require alternative substrates to sustain metabolic reactions (Araujo et al., 2011). Such energetic demands may require the disassembly of organellar components and the redirection of alternative substrates for respiration. In plants, the major protein reserve is in the chloroplast, as approximately 80% of the total leaf nitrogen corresponds to photosynthetic proteins in C3 plants (Ishida et al., 2008). The degradation of chloroplasts is a hallmark of both natural and stress-induced plant senescence, and their catabolic products are used for energy production during carbon starvation conditions (Wada et al., 2009; Izumi et al., 2013, 2017, 2018). Accordingly, autophagy plays a key role in this process by targeting chloroplast proteins for degradation (Ishida et al., 2008; Xie et al.,2015; Izumi et al.,2017, 2018; Hirota et al., 2018).

Overall, autophagy is a well-characterized pathway by which cytoplasmic components are engulfed and delivered by a specialized double-membrane structure (autophagosome) to the vacuole for recycling (Michaeli et al., 2016; Magen et al., 2022). Interestingly, several autophagy-mediated chloroplast degradation pathways are differentially activated under distinct conditions (Izumi et al., 2018). The encapsulation of entire chloroplasts into ATG8-decorated autophagic vesicles and their subsequent delivery to the vacuole is termed "chlorophagy". This process is dependent on ATG8 lipidation and is induced upon UV-B or high-light treatments (Izumi et al. , 2017; 2018). Rubisco-containing bodies (RCBs) are part of another type of chloroplast autophagy that provides piecemeal transport of stromal proteins, and is activated upon carbohydrate starvation (Ishida et al. 2008; Izumi et al., 2018; Hirota et al., 2018). By contrast, ATI (ATG8-Interacting 1) bodies, a type of chloroplast autophagy relying on a specific ATG8-binding protein, are initiated inside the chloroplast being associated with thylakoid, envelope, and stroma proteins (Michaeli et al., 2014; 2016). The appearance of plastid-associated ATI bodies has been observed in both senescent leaves and energy-starved seedlings (Michaeli et al., 2014; 2016).

Recent studies have also highlighted the relevance of autophagy-independent chloroplast degradation mechanisms, namely the Senescence Associated Vacuoles (SAVs) and Chloroplast Vesiculation (CV). SAVs are small proteolytic vacuolar compartments that degrade a subset of chloroplast components and accumulate in senescing leaves (Otegui et al., 2005; Martínez et al., 2008; Gomez et al., 2019). SAVs have been shown

to contain stromal proteins and exhibit strong cysteine protease activity, as evidenced by the presence of the senescence-associated protease *SAG12* (Otegui et al., 2005). In addition, CV was characterized as a chloroplast degradation pathway independent of either SAVs or autophagy (Wang and Blumwald, 2014). It was first described in rice as being strongly upregulated under abiotic stress and downregulated by cytokinin (Peleg et al., 2011). Later on, using Arabidopsis mutants, CV-containing vesicles (CCVs) were characterized as mobilizing thylakoid and stromal proteins to the vacuole for degradation (Wang and Blumwald, 2014). Furthermore, the disruption of CV has been associated with increased chloroplast stability, a delay in dark induced-senescence, and an enhanced tolerance to abiotic stress, whereas by contrast its overexpression results in premature leaf senescence (Wang and Blumwald, 2014; Sade et al., 2018; Ahouvi et al., 2022; Yu et al., 2022). In addition, a role for CV in mediating peroxisomal turnover and thereby contributing to the regulation of photorespiration and N assimilation in rice under elevated CO_2, was also reported (Umnajkitikorn et al., 2020).

Although our knowledge of chloroplast degradation pathways has increased greatly during the last decade, the molecular hierarchy of these diverse pathways remains to be elucidated. Autophagy plays a key role in chloroplast degradation events, yet *atg* mutants have been shown to undergo early leaf senescence and accelerated degradation of chloroplast components upon diverse stress conditions (Thompson et al., 2005; Lee et al., 2013; Izumi et al., 2013; Barros et al., 2017, 2021; Hirota et al., 2018). These observations argue against a major role of autophagy in chloroplast degradation during senescence and highlight a possible connection between the different chloroplast degradation processes in response to stresses. In this context, we previously observed that the *CV* gene is highly induced in the absence of autophagy, contributing to the early-senescence phenotype observed in *atg5* and *atg7* mutants (Barros et al., 2017). Nevertheless, it remains unclear to which extent these pathways interact to control chloroplast stress responses.

Here, we investigated the significance of the CV pathway during carbon starvation. To this end, two previously described mutant lines with low expression of the CV pathway (*amircv-1* and *amircv-2*) were characterized under dark-induced senescence conditions. Our results demonstrate that deficiency of CV alone only has minor effects on plant responses to extended darkness. We further assessed the relationship between CV and autophagy by analyzing *amircv1xatg5* double-mutant plants that are characterized by a deficiency in both pathways. Although the *amircv1xatg5* double mutants displayed a hypersensitive phenotype, similar to that observed in *atg5* mutants under late stages of darkness, both CV and autophagy are likely required for chloroplast remodeling during these conditions. Our results further support the notion that autophagy is the preferred mechanism of chloroplast turnover under carbon-limiting conditions, while CV likely operates as a compensatory mechanism when autophagy is disrupted.

RESULTS

Phenotypes of *amircv* mutant lines

To examine the metabolic consequences of CV impairment, we used two previously described micro-RNA mutants lines, namely *amircv-1* and*amircv-2* (Wang and Blumwald 2014). The low expression of the*CV* gene was initially confirmed by RT-qPCR (Supplemental Fig. S1). We next investigated the physiological consequences of CV impairment under optimal conditions. Photosynthetic parameters were determined in mature plants of *amircv* mutants and WT grown under short-day conditions. No differences were observed in net assimilation rate (Fig. 1A), stomatal conductance (Fig. 1B), and internal CO_2 concentration (Fig. 1C) of *amircv-1* and*amircv-2* lines compared to WT. This result is in line with previous data, demonstrating that the CV pathway functions in chloroplast degradation mainly under abiotic stress (Wang and Blumwald 2014; Sade et al., 2018; Ahouvi et al., 2022). Accordingly, rice and tomato *CV* knockdown mutants exhibited higher photosynthesis rates only when submitted to water and salt stress, while similar photosynthetic rates were observed under optimal conditions (Sade et al., 2018; Ahouvi et al., 2022).

Given that the induction of the *CV* gene during energy depletion conditions has been previously demonstrated (Barros et al., 2017, 2022; Yu et al., 2022), we next transferred 4-week-old plants to extended darkness, a system previously used to prove the metabolic importance of autophagy and alternative pathways of re-

spiration in plants (Ishizaki et al., 2005; Araújo et al., 2010; Barros et al., 2017). After 10d of continuous darkness, both WT and *amircv* plants exhibited only limited signs of leaf senescence (Fig. 2A). To obtain a detailed analysis of leaf senescence parameters, we measured the total chlorophyll content and the maximum variable fluorescence/maximum yield of fluorescence (F v/F m). Chlorophyll loss coupled with reductions of F v/F m were observed throughout the experiment (Fig. 2B and C). In agreement with the visual phenotype reported, no significant differences in chlorophyll levels and$F$ v/F m were verified in *amircv* lines under extended darkness conditions.

Down-regulation of *CV* has minor effects on starvation response

To elucidate the role of the CV pathway in plant energetic metabolism, we further conducted a metabolic characterization of *amircv*plants. Thus, the levels of starch, protein, sugars, and organic acids were determined (Fig. 3). As might be expected, sugars (sucrose, fructose, and glucose) and starch declined rapidly from 3d of dark treatment in all genotypes (Fig. 3A-D). Both fumarate and malate were initially reduced in WT and the *amircv* lines at 3d. Fumarate levels were further slightly increased throughout the darkness treatment (Fig. 3E-F). This result is in accordance with the dual pattern of TCA cycle intermediates commonly observed during extended darkness conditions (Ishizaki et al., 2005; Araújo et al., 2010; Barros et al., 2017; Kamranfar et al., 2018). During both developmental and induced senescence, plant cells undergo massive changes in cellular metabolism and activate progressive hydrolysis of macromolecules (Watanabe et al., 2013; Sade et al., 2018). Besides sugars, catabolism of proteins, lipids, and chlorophyll provides energetic substrates that allow the continued operation of mitochondrial respiration (Araújo et al., 2011; Hortensteiner & Krautler, 2011; Barros et al., 2020). Accordingly, following the exhaustion of carbohydrate reserves, during extended darkness, a drop in protein content was observed (Fig. 3G). It is worth mentioning that the *amircv* mutants presented a slightly higher reduction of protein content in the early stage of darkness. Protein degradation during stress conditions and senescence leads to a generally increased amino acid accumulation (Araujo et al., 2011; Watanabe et al., 2013). Consistently, the enhanced protein degradation resulted in a slight increase of total amino acids in the *amircv* mutants after 3d of darkness (Fig. 3H). Despite this, the *amircv* lines and WT presented relatively similar metabolic responses throughout the darkness treatment.

Amino acids are the main alternative substrates to provide energy to alternative respiration pathways under carbon starvation (Ishizaki et al., 2005,2006; Araújo et al.,2010,2011; Cavalcanti et al., 2017). More specifically, branched-chain amino acids (BCAA) and lysine have been extensively reported to participate in energy generation by the alternative pathway mediated by the ETF-ETFQO system (Araújo et al., 2010, 2011). We previously demonstrated that both CV and alternative respiratory pathways are activated in autophagy mutants submitted to extended darkness (Barros et al., 2017). Thus, to investigate the interplay between these processes, the expression of selected genes related to alternative respiration, BCAA, and lysine degradation was investigated in the *amircv* mutants (Fig. 4). This analysis revealed that the *ETFQO* gene is induced during the darkness treatment (Fig. 4A). In a similar vein, the transcript levels of*IVDH* , a key enzyme of BCAA degradation, was also up-regulated under these conditions (Fig. 4B). The induction of *ETFQO* and BCAA catabolism related genes during low energy and senescence conditions have been extensively reported previously (Izumi et al., 2013, Chrobok et al., 2016; Barros et al., 2017,2022; Hirota et al., 2018). Nevertheless, similar induction of *ETFQO* and *IVDH*transcripts was observed in WT and *amircv* mutant plants. Furthermore, we analyzed the Lys-ketoglutarate reductase/saccharopine dehydrogenase (*LKR/SDH*) gene, which encodes a key enzyme of lysine catabolism. A strong induction of *LKR/SDH* was observed during darkness in all genotypes, with a trend of minor induction of*LKR/SDH* in the *amircv* mutants after 10d of darkness (Fig. 4C). The enzyme LKR/SDH controls most of the lysine homeostasis, presenting a complex regulation both at the transcriptional and post-translational level (Arruda and Barreto, 2020). It was recently reported that both *CV* and *LKR/SDH* are activated during aging and abiotic stress by a common regulator, the RD26 transcription factor (Kamranfar et al., 2018). Additional studies are required to understand the possible connection between CV and lysine metabolism. However, our results collectively suggest that *CV* downregulation exerts a minor influence on the activation of energetic amino acid catabolism and ETF/ETFQO pathways during extended darkness conditions.

Deficiency of CV and Autophagy trigger susceptibility to extended darkness

Taking into account that autophagy has a recognized role in plant energetic homeostasis under carbon starvation conditions (Ishida et al., 2013; Barros et al., 2017,2021; Hirota et al., 2018; McLoughlin et al., 2020), we further evaluated the autophagic process in the *amircv*plants. For this purpose, we measured the transcript levels of*ATG8h* , which encodes an isoform of the ATG8 protein required for autophagosome elongation. These increased from 3d of darkness in both WT and *amircv* mutants (Fig. 4D), suggesting a general activation of autophagy under these conditions. It was previously reported that CV and autophagy are independent pathways, occurring concomitantly in the cell (Wang and Blumwald, 2014). The lack of CV does not trigger any differential autophagy activation under extended darkness. However, the*CV* gene is upregulated in plants lacking autophagy during darkness treatment (Barros et al., 2017). Thus, our results suggest that CV triggers minor effects on energetic metabolism when autophagy is functional.

To test the coordination of these two pathways, we next generated double mutants for both CV and autophagy: *amircv1* x*atg5* (Fig. 5A). Double mutant plants and their parental lines were grown side-by-side under short-day and further submitted to extended darkness conditions. Interestingly, after 10d of darkness, the double mutants exhibited an early senescence phenotype similar to the *atg5* single mutant (Fig. 5B). The sensitivity phenotype observed in both *atg5* and*amircv1* x*atg5* mutants was followed by a massive reduction of chlorophyll levels (Fig. 5C). Since the sensitive phenotype was not recovered in *amircv1* x*atg5* mutants, it seems reasonable to suggest that other chloroplast catabolic pathways are likely activated in both *atg5* and *amircv1xatg5* plants under darkness.

Effects of autophagy and CV deficiency on metabolic adjustment under extended darkness

To gain more insight into the differential impacts of CV and autophagy deficiency under extended darkness, we further analyzed the metabolic profile of *amircv1xatg5* along with its parental lines,*amircv-1* and *atg5* (Fig. 6 and 7). In agreement with the phenotype observed, *amircv-1* presented similar metabolic changes to WT plants, while *atg5* and a*mircv1xatg5* exhibited more comparable responses. While the majority of amino acids were highly accumulated in WT and *amircv-1* plants, only minor accumulations of arginine, glutamate, glycine, isoleucine, lysine, serine, threonine and valine were observed in *atg5* and *amircvxatg5* after 10d of extended darkness (Fig. 6). We also found that the TCA cycle intermediates α-ketoglutarate, citrate, fumarate, malate, and succinate were highly accumulated in both *atg5* and *amircvxatg5*mutants after 10d of darkness (Fig. 7). These results are consistent with previous findings demonstrating the impairment of amino acid provision coupled with an altered respiratory response in *atg*mutants under extended darkness (Barros et al., 2017; Hirota et al., 2018).

Despite the similarities with the *atg5* mutant,*amircv1xatg5* also showed specific metabolic signatures. The general accumulation of organic acids was lower in the*amircv1xatg5* mutant compared to the *atg5* mutant after 10d of darkness (Fig. 7). Additionally, the *amircv1xatg5* mutant displayed lower accumulation of arginine, aspartate, glutamate, isoleucine, serine and valine levels in the later stages of darkness (Fig. 6). Glutamate, glutamine, asparagine, aspartate are important components of nitrogen assimilation, recycling, transport and storage in plants (Gaufichon et al., 2010). The coordination between CV and nitrogen assimilation pathways was previously proposed during water stress and elevated CO_2 conditions wherein rice CV mutants presented altered levels of amino acids (Sade et al., 2018; Umnajkitikorn et al., 2020). On the other hand, the disruption of autophagy impacts the supply of amino acids and respiratory rates under carbon depletion (Izumi et al., 2013; Avin-Wittenberg et al., 2015; Barros et al., 2017; Hirota et al., 2018). Collectively, our results indicate that a deficiency solely of CV has only minor effects on plant responses to extended darkness, and suggests that the metabolic reprogramming of *atg5* mutants under extended darkness is, at least partially, dependent on the operation of a functional CV pathway.

CV contributes to the abnormal chloroplast structure of*atg5* mutants under extended darkness

Given that both autophagy and CV can mediate chloroplast degradation, we next used transmission electron microscopy to investigate the effects of a simultaneous lack of autophagy and CV on chloroplast structure. Before darkness treatment, chloroplasts of all the genotypes appeared undamaged at the ultrastructural level,

containing large starch granules, grana, stroma thylakoids and occasionally occurring small plastoglobules (Fig. 8A-D). After 7d of darkness, WT and the single mutant *amircv-1* chloroplasts displayed similar structures, containing remodeled thylakoid systems and granal stacking (Fig. 8E-F). However, the membrane organization of the *amircv1* x*atg5* chloroplasts was notably disturbed (Fig. 8H). We previously showed that *ATG5* mutation compromises chloroplast integrity under darkness (Barros et al., 2021). Interestingly, when comparing the *atg5* and *amircv1xatg5* mutants, differential changes in chloroplast structure were observed (Fig. 8G and H). In addition to the marked supersized plastoglobuli, *atg5* chloroplasts lost their normal structure exhibiting a longish and curved shape containing deformed stroma and several vesicles (Fig. 8G). These vesicle structures resemble senescence-associated vacuoles (SAVs), which also mediate the recycling of chloroplast proteins by an autophagy-independent mechanism (Otegui et al., 2005). Additionally, the *atg5* chloroplasts lost the curved thylakoid membrane response observed in WT and the *amircv-1* genotypes. Despite the presence of granal stacking in *atg5* , the granum was narrow with more layers (Fig 8I and L). On the other hand, it seems that the *amircv1xatg5* chloroplasts partially recovered the curved thylakoid membrane response, yet the of granal structure was highly compromised compared to WT and single mutants (Fig 8H and M). It is generally accepted that chloroplast stacking is governed by physicochemical forces between membranes and lipid-protein interactions (Armbruster et al., 2013; Johnson and Wientjes, 2019; Mazur et al., 2019). Since CV and autophagy operate in the selective degradation of chloroplast proteins, it is tempting to suggest that the distinct chloroplast responses observed are likely associated with differential protein degradation in these genotypes.

DISCUSSION

To cope with energetically challenging conditions, plants activate strategic mechanisms of organelle disassembly, which generally culminate in a senescence-induced response. During both developmental and stress-induced senescence, chloroplast proteins are massively degraded, and the amino acids released can be either remobilized for other tissues or used as respiratory substrates (Araujo et al., 2011, Watanabe et al., 2013, Hildebrandt et al., 2015; Chrobok et al., 2016). It is well known that chloroplasts contain their own proteolytic machinery, comprising several types of proteases that operate in their protein quality control (Buet et al., 2019). This fact aside, recent studies have reported the existence of extra-plastidial pathways for chloroplast turnover (Otegui 2017; Izumi and Nakamura, 2018; Woodson 2022). Three main extra-plastidic processes involved in the degradation of chloroplasts were identified: autophagy (Ishida et al., 2008; Wada et al., 2009), SAVs (Otegui et al., 2005; Martínez et al., 2008), and CV (Wang and Blumwald, 2014). It remains unknown, however, how these distinct pathways are regulated and under which molecular hierarchy they ensure proper chloroplast turnover. We previously suggested that CV might function as a compensatory mechanism contributing to the sensitive phenotype of *atg* mutants under carbon starvation (Barros et al., 2017). Here, we provide additional experimental evidence of the importance of CV and autophagy pathways for both metabolic responses and chloroplast remodeling under extended darkness.

We first investigated the effects of the disruption of CV alone, on plant tolerance to extended darkness. Thus, we focused on phenotypic and metabolic characterization of previously described mutant lines exhibiting deficient expression of the *CV* gene (Wang and Blumwald, 2014). Accordingly, we verified that WT and *amircv-1* and *amircv-2* plants displayed similar phenotypes under conditions of extended darkness (Fig. 2). However, the reduced protein content coupled with an elevated total free amino acid level after 3d of darkness indicates that mechanisms of protein turnover are more rapidly induced in the *amircv* mutants (Fig. 3). Furthermore, minor metabolic differences were observed between the *amircv* mutants and WT plants throughout the darkness treatment (Fig. 3 and 6). Additionally, the accumulation of amino acids was not correlated with differential activation of alternative respiration pathways in the *amircv* lines (Fig. 4). Collectively, these findings suggest that the altered protein response observed in the *amircv* mutants does not trigger significant effects on energetic metabolism.

It was previously demonstrated that silencing CV resulted in increased chloroplast stability, whereas CV overexpression led to chloroplast degradation by destabilizing the photosynthetic apparatus during abiotic stress (Wang and Blumwald, 2014; Sade et al., 2018; Ahouvi et al., 2022; Yu et al., 2022). By contrast,

plants with enhanced autophagy were fitter and displayed enhanced tolerance to oxidative stress (Minina et al., 2018). Autophagy is a versatile mechanism of chloroplast degradation since it mediates the turnover of piecemeal stroma components and the degradation of entire chloroplasts by the chlorophagy mechanism (Izumi and Nakamura, 2018). Experimental evidence has suggested that the selective degradation of stromal proteins mediated by autophagy, the RCB pathway, is preferentially activated to provide amino acids in energy-starved plants (Hirota et al., 2018; Izumi et al., 2019). Taken together, the data described above, coupled with our results, suggest that autophagy is more likely to operate as a pro-survival mechanism by the turnover of stromal components under starvation conditions, while CV leads to the widespread degradation of chloroplasts under specific abiotic stress conditions. Additionally, our previous study indicated a higher activation of the CV pathway in*atg* mutants submitted to extended darkness (Barros et al., 2017). Therefore, it is tempting to suggest that autophagy operates as a primary chloroplast degradation pathway, while CV is most likely a complementary mechanism activated in the absence of autophagy. By contrast, a recent study revealed that CV-silenced tomato plants display stable chloroplast structure, ROS control, and delayed senescence in response to extended darkness (Yu et al., 2022). Therefore, these results open new questions regarding possibly contrasting roles of CV in metabolic reprogramming in different plant species under starvation conditions.

To unravel how these pathways modulate chloroplast turnover and stress-induced senescence response, we further characterized double mutants for both CV and autophagy pathways. Surprisingly, under extended darkness, these *amircv1xatg5* mutants displayed an early senescence response accompanied by a reduction of chlorophyll levels, resembling the *atg5* single mutant phenotype (Fig. 5). The metabolic analysis also demonstrated that tCV deficiency alone only resulted in minor effects on metabolic reprogramming, whereas the disruption of both autophagy and CV triggered similar effects as deficiency in*atg* alone(Fig. 6 and 7). Nevertheless, levels of specific amino acids differed between *amircv1xatg5* and *atg5*mutants. The *amircv1xatg5* double mutants displayed more reduced levels of arginine, aspartate, glutamate, isoleucine, serine and valine after 10d of darkness compared to the *atg5* mutants (Fig. 6). Glutamine, glutamate, asparagine, aspartate, and their derivatives have been long documented to be key compounds of nitrogen metabolism (Masclaux-Daubresse et al., 2006; Gaufichon et al., 2016). The fact that the *amircv1xatg5* mutant displayed reduced levels of arginine, aspartate and glutamate suggests a possible impairment of N remobilization pathways in the *amircv1xatg5* mutants. Interestingly, the link between CV and N assimilation was previously observed in rice CV mutants under water stress (Sade et al., 2018). Under this condition, RNAiOsCV plants were characterized by altered expression of N metabolism genes and differential activity of nitrate reductase (NR) and glutamate dehydrogenase (GDH). It was additionally demonstrated that CV interacts with glutamine synthase 2 (GS2) mediating its degradation. Altogether these results were associated with the activation of N assimilation in RNAi*Os* CV plants ensuring a superior performance under water stress (Sade et al., 2018).

In the context of darkness-induced carbon starvation , the shift in amino acid metabolism by CV deficiency is likely capable of compromising plant survival, once amino acids are extensively used as energetic substrates under these conditions. Indeed, the impairment of amino acid release in *atg* mutants leads to energetic failure and differential respiratory response under extended darkness conditions (Barros et al., 2017). Interestingly, the *amircv1xatg5* mutants displayed ed lower accumulation of TCA cycle intermediates compared to the *atg5* single mutant (Fig. 7). Our previous study associated the higher levels of organic acids to a higher flux through the tricarboxylic acid cycle as a consequence of the respiratory activity in Arabidopsis *atg* mutants (Barros et al., 2017). The accumulation of TCA cycle intermediates during dark and developmental senescence has previously been suggested as a symptom of higher respiration (Araujo et al., 2010, 2011). In this context, the minor increases of organic acids observed in the *amircv1xatg5* mutant suggest that the respiratory activation of the *atg5* mutant is somehow restrained in the absence of CV. In addition to chloroplasts, it has been shown that CV is also important in peroxisome and possibly mitochondrial maintenance. In this context, the OsCV rice mutant was characterized by a reduced number of peroxisomes and mitochondria under elevated CO_2levels (Umnajkitikorn et al., 2020). Accordingly, the activation of OsCV mediates the removal of the OsPEX11 protein to the vacuole, triggering a reduced number of peroxisomes and decreased catalase activity under elevated CO_2 conditions (Umnajkitikorn et al., 2020). The role of CV in peroxi-

somal protein turnover was also demonstrated in tomato plants submitted to extended darkness wherein SlCV interacts with SlCAT3 leading to excessive accumulation of ROS (Yu et al., 2022). Considering that energy-related pathways occur in different cell compartments, it may be expected that CV participates in the maintenance/degradation of other organelles in addition to chloroplasts. Therefore, the reduced levels of TCA cycle intermediates in the double mutants may also be triggered by a possible differential degradation of peroxisome and mitochondria in the *amircv1xatg5* mutants. The accumulation of peroxisome and mitochondrial proteins in *atg*mutants has been extensively investigated (Shibata et al., 2013; Yoshimoto et al., 2014; Li et al., 2014; Ma et al, 2021; Kacprzak and van Aken, 2022). Despite that, the exact connection between CV and autophagy in maintaining energy-related organelles still needs to be addressed.

To decipher the importance of autophagy and CV pathways in chloroplast maintenance, we paid particular attention to the analysis of chloroplast ultrastructure. It was previously reported that *atg5* mutants presented marked changes in chloroplast structure following extended darkness conditions (Barros et al., 2021). Here, we further demonstrated that the disruption of both CV and autophagy leads to a differential chloroplast ultrastructure under extended darkness. Accordingly, the*atg5* mutant displayed deformed chloroplasts with a more compromised stromal structure (Fig. 8). Although we observed certain conservation of grana in the chloroplasts of the *atg5* mutants, the thylakoid membrane system was static and missed the typical reorganization of darkened chloroplast observed in the WT and*amircv-1* lines, characterized by curvature of thylakoid membranes. On the other hand, the*amircv1xatg5* chloroplasts partially recovered thylakoid membrane organization, despite showing compromised granal stacking (Fig. 8). It was previously observed that *CV* overexpression induced chloroplast structural changes, characterized by the unstacking and swelling of the thylakoid membranes which compromised chloroplast stability (Wang and Blumwald, 2014; Yu et al., 2022). Interestingly, our results show that downregulation of CV combined with the absence of autophagy results in more compromised thylakoid and grana structures compared to WT and to the correspondent single mutants under extended darkness. It is worth mentioning that CV was previously proposed to mediate the target of PsbO protein, altering the structure of the photosystem II, and facilitating the access of the thylakoid-associated proteases, such as DEGP1 and FTSH, to chloroplast core proteins (Wang and Blumwald, 2014). The lack of chloroplast repair mediated by proteases results in the accumulation of damaged chloroplast proteins, generating ROS (Kato and Sakamoto et al., 2009), and possibly thereby leading to the deregulation of chloroplast machinery. Therefore, it is tempting to suggest that the selective turnover of envelope proteins by the CV pathway contributes to chloroplast remodeling in the absence of autophagy. It should also be highlighted that lipid composition directly influences the biophysical properties of thylakoid membranes (Mazur et al., 2019). Indeed, recent studies have reported massive changes in galactolipids in plants lacking autophagy (Have et al., 2019; McLoughlin et al., 2020; Barros et al., 2021). However, the potential roles of CV in chloroplast lipid composition remain to be addressed.

Collectively, the findings described here refine our understanding of chloroplast degradation events during dark-induced senescence. By contrast to the situation observed when autophagy is disrupted, the impairment of CV has a minor impact on plant response to energy deprivation. This highlights the preferential activation of autophagy-mediated pathways to ensure chloroplast maintenance and starvation response under extended darkness. Our data further suggest that CV deficiency triggers minor energetic consequences when autophagy is still present and activated. The further characterization of*amircv1xatg5* double mutants revealed a potential role of CV in the metabolic response and chloroplast remodeling of the *atg5*mutant during extended darkness. Noteworthy, the early senescence phenotype of the *amircv1xatg5* mutants under extended darkness highlights the possible operation of other catabolic pathways. The presence of SAVs in *atg5* chloroplast indicates the relevance of this pathway in chloroplast turnover during these conditions. Dissecting the intertwined mechanisms regulating chloroplast turnover are still required to fully understand the exact relation between autophagy, CV and SAVs on chloroplast maintenance and plant stress tolerance.

METHODS

Plant material and dark treatment

Two *Arabidopsis* RNAi mutant lines for *CV* gene,*amircv-1* and *amircv-2* (Wang and Blumwald, 2014), the T-DNA line *atg5-1* (SAIL_129B079) and its correspondent WT (Columbia 0 ecotype) were used in this study. Seeds were surface-sterilized and imbibed for 4 days at 4degC in the dark and subsequently germinated. Seedlings grown at 22degC under short-day conditions (8 h light/16 h dark), 60% relative humidity with 150 µmol photons m^{-2} s^{-1}. *amircv* mutants were selected by application of Glufosinate-ammonium (120 mg/L) in ten-old day seedlings. For dark treatments, selected seedlings were grown at 22°C under short-day for 4 weeks. Afterwards, plants were maintained in dark in the same growth cabinet. The rosettes were harvested at intervals of 0, 3, 7 and 10 days after transition to darkness and immediately frozen in liquid nitrogen and stored at -80°C until further analysis.

Measurements of photosynthetic parameters

Gas-exchange measurements were performed with an open-flow infrared gas-exchange analyzer system (Li-Cor 6400XT) with a portable photosynthesis system. Light was supplied from a series of light-emitting diodes located above the cuvette, providing an irradiance of 150 µmol photons m^{-2} s^{-1}, similar to the growth conditions aforementioned. The reference CO_2 concentration was set at 400 mmol CO_2 mol^{-1} air. All measurements were performed at 25°C, and the vapor pressure deficit was maintained at 0.2 kPa, while the amount of blue light was set to 10% of photon flux density to optimize stomatal aperture. The determination of the photosynthetic parameters was performed in 4-week-old plants.F v/F m, which corresponds to the potential quantum yield of the photochemical reactions of PSII and represents a measure of photochemical efficiency, was measured as described previously (Oh et al., 1996).

Biochemical assays

Leaf samples were harvested at the time points indicated, immediately frozen in liquid nitrogen, and stored at -80°C until further analysis. Extraction was performed by rapid grinding of tissue in liquid nitrogen and the immediate addition of ethanol as described in Gibon et al. (2004). Photosynthetic pigments were determined as in Porra et al. (1989). The levels of starch, sucrose, glucose, and fructose were determined exactly as described previously (Fernie et al., 2001). Malate and fumarate contents were determined as described before (Nunes-Nesi et al., 2007). Protein and amino acid contents were determined as described previously (Cross et al., 2006).

Metabolite profiling

Metabolite extraction was performed essentially by following an established gas chromatography-mass spectrometry (GC-MS)-based metabolite profiling protocol of Lisec et al. (2006) modified. Approximately 50 mg of homogenized plant materials were aliquoted in tubes and extracted in 100% methanol and internal standard (0.2 mg ribitol mL^{-1} water). 2.0 mL tubes were shaken for 15 min at 70°C and next centrifuged at 11000g for 10 min. The supernatant was transferred to new tubes and, afterwards, 100% chloroform and distilled water were added. Tubes were centrifuged at 2200 gfor 15 min. Finally, 150 µL of the upper phase of each sample were transferred to new 1.5 mL tubes and left to dry overnight in a vacuum concentrator. Sample derivatization was carried out as previously described (Lisec et al., 2006). A pooled reference sample was made by combining 5 µl aliquots from all samples. Sample injection and subsequent peak annotation were performed as described in Dahtt et al. (2019), using the Fiehn GC/MS Metabolomics RTL Library (G1676AA; Agilent). After blank subtraction, the peak area of each metabolite was normalized to the internal standard (i.e., ribitol) in each sample, as well as fresh weight.

Expression analysis by RT-PCR

Total RNA was isolated using TRIzol reagent (Ambion, Life Technology) according to the manufacturer's recommendations. The total RNA was treated with DNAse I (RQ1 RNase free DNase I, Promega, Madison,

WI, USA). The integrity of the RNA was checked on 1% (w/v) agarose gels, and the concentration was measured using a Nanodrop spectrophotometer. Finally, 2 µg of total RNA were reverse transcribed with Superscript II Rnase H2 reverse transcriptase (Invitrogen) and oligo (dT) primer according to the manufacturer's recommendations. Real-time PCR reactions were performed in a 96-well microplate (Applied Biosystems Applera, Darmstadt, Germany), using Power SYBR Green PCR Master Mix. The primers used here were designed using the open-source program QuantPrime-qPCR primer designed tool (Arvidsson et al., 2008) and are described in Table S2. ACTIN (AT2G37620) was used as internal standard. The relative levels of mRNAs were determined using the $2^{-\Delta^{\circ}\tau}$ method (Livak and Schmittgen, 2001). Three biological replicates were processed for each experimental condition.

Transmission Electron Microscopy

Small pieces of leaves were cut and fixed in 3% Glutaraldehyde in 0.1M Cacodylate buffer (pH 7.4) for 10 hours at room temperature in a desiccator and then transferred to 40° C for a continuation of fixation overnight. Tissues were washed in cacodylate buffer and post-fixed and stained with 2% osmium tetroxide, and 1.5% potassium ferricyanide in 0.1M cacodylate buffer for 2 hours. Tissues were then washed in cacodylate buffer and dehydrated through a graded series of ethanol treatments for 10 min each step followed by 100% anhydrous ethanol 3 times, 20 min each, and propylene oxide 2 times, 10 minutes each. The tissues were infiltrated with increasing concentrations of Agar 100 resin in propylene oxide for 16 hours at each step. The tissues were embedded in fresh resin at 60°C oven for 48 hours. Ultrathin sections, approximately 80 nm thick, were cut on a Leica Reichert Ultracut S microtome, collected onto 200 Mesh carbon-formvar coated copper grids and stained with Uranyl acetate followed by Reynold's Lead Citrate for 10 min. The sections were examined using Tecnai 12 TEM 100kV (Phillips, Eindhoven, the Netherlands) equipped with MegaView II CCD camera and Analysis® version 3.0 software (SoftImaging System GmbH, Münster, Germany).

Statistical analyses

The experiments were conducted in a completely randomized design with 3-5 replicates of each genotype. Data were statistically examined using analysis of variance and tested for significant (P [?] 0.05) differences using Student's t test. All statistical analyses were performed using the algorithm embedded into Microsoft Excel.

ACKNOWLEDGEMENTS

The authors would like to acknowledge Dr. Edward Blumwald (University of California) for sharing the *amircv* seeds used in this work. We also thank Dr. Yael Friedmann from the microscopy core facility at The Hebrew University's Life Science core facility for her technical support with confocal and EM analysis. This work was supported by funding from the National Council for Scientific and Technological Development (CNPq-Brazil,Grant 407276/2021-1), the National Institute of Science and Technology in Plant Physiology under Stress Conditions (INCT Plant Stress Physiology/CNPq-Brazil /Grant 406455/2022-8),) and the FAPEMIG (Foundation for Research Assistance of the Minas Gerais State, Brazil, Grant RED-00053-16). Work at the TAW group is supported by the Israeli Science Foundation, grant number 1899/16. Scholarships granted by the National Council for Scientific and Technological Development (CNPq-Brazil) and Council for Higher Education (Malag-Israel) to JASB and research fellowships awarded by CNPq-Brazil to ANN and WLA are also gratefully acknowledged.

Authors contribution

J.A.S.B., J.H.F.C., T.A-W., and W.L.A. designed the research; J.A.S.B. performed most of the research with the support of J.H.F.C, S.M, D.B.M, and K.G.P; T.A-W. and W.L.A. supervised the project; K.G.P contributed with mutants obtention and confirmation, T.A-W and S.M and Y.S performed metabolite profiling; A.N-N. and A.R.F. contributed with new reagents/analytic tools; J.H.F.C, D.B.M., A.N-N, and A.R.F. discussed the results and complemented the writing. J.A.S.B., T.A-W., and W.L.A. analyzed the data and wrote the article, which was later approved by all the others.

REFERENCES

Ahouvi Y, Haber Z, Zach YY, Rosental L, Toubiana D, Sharma D, Alseekh S, Tajima H, Fernie AR, Brotman Y, Blumwald E, Sade N (2022). The Alteration of Tomato Chloroplast Vesiculation Positively Affects Whole-Plant Source–Sink Relations and Fruit Metabolism under Stress Conditions. Plant and Cell Physiology, https://doi.org/10.1093/pcp/pcac133

Araujo WL, Ishizaki K, Nunes-Nesi A, Larson TR, Tohge T, Krahnert I, Witt S, Obata T, Schauer N, Graham IA, Leaver CJ, Fernie AR(2010) Identification of the 2-hydroxyglutarate and isovaleryl-CoA dehydrogenases as alternative electron donors linking lysine catabolism to the electron transport chain of Arabidopsis mitochondria. Plant Cell**22:** 1549-1563.

Araujo WL, Tohge T, Ishizaki K, Leaver CJ, Fernie AR (2011) Protein degradation - an alternative respiratory substrate for stressed plants. Trends in Plant Science **16:** 489–498.

Armbruster U, Labs M, Pribil M, Viola S, Xu W, Scharfenberg M, Hertle AP, Rojahn U, Jensen PE, Rappaport F, et al (2013) Arabidopsis CURVATURE THYLAKOID1 proteins modify thylakoid architecture by inducing membrane curvature. Plant Cell **25** : 2661–2678

Arruda P, Barreto P (2020) Lysine catabolism through the saccharopine pathway: enzymes and intermediates involved in plant responses to abiotic and biotic stress. Front. Plant Sci. **11:**587

Arvidsson S, Kwasniewski M, Riano-Pachon DM, Mueller-Roeber B(2008) QuantPrime: flexible tool for reliable high-throughput primer design for quantitative PCR. BMC Bioinformatics **9** : 465

Avin-Wittenberg T, Bajdzienko K, Wittenberg G, Alseekh S, Tohge T, Bock R, Giavalisco P, Fernie AR (2015) Global analysis of the role of autophagy in cellular metabolism and energy homeostasis in Arabidopsis seedlings under carbon starvation. Plant Cell **27** : 306–322

Barros JAS, Cavalcanti JHF, Medeiros DB, Nunes-Nesi A, Avin-Wittenberg T, Fernie AR, Araujo WL(2017) Autophagy deficiency compromises alternative pathway of respiration following energy deprivation. Plant Physiol **175** : 62–76

Barros JAS, Siqueira JAB, Cavalcanti JHF, Araujo WL, Avin-Wittenberg T (2020) Multifaceted Roles of Plant Autophagy in Lipid and Energy Metabolism. Trends Plant Sci.**25 (11):** 1141-1153

Barros JAS, Magen S, Lapidot-Cohen T, Rosental L, Brotman Y, Araujo WL, Avin-Wittenberg T(2021) Autophagy is required for lipid homeostasis during dark-induced senescence. Plant Physiol **185** : 1542–1558

Barros JAS, Cavalcanti JHF, Pimentel KG, Medeiros DB, Silva JCF. Condori-Apfata JA, Lapidot-Cohen T, Brotman Y, Nunes-Nesi A, Fernie AR, Avin-Wittenberg T, Araujo WL (2022) The significance of WRKY45 transcription factor in metabolic adjustments during dark-induced leaf senescence. Plant, Cell & Environment **45** : 2682– 2695.https://doi.org/10.1111/pce.14393

Buet A; Costa ML; Martinez DE; Guiamet JJ (2019) Chloroplast protein degradation in senescing leaves: Proteases and lytic compartments. Front. Plant Sci. **10** : 747

Cavalcanti JHF, Quinhones CGS, Schertl P, Brito DS, Eubel H, Hildebrandt T, Nunes-Nesi A, Braun H-P, Araujo WL (2017) Differential impact of amino acids on OXPHOS system activity following carbohydrate starvation in Arabidopsis cell suspensions. Physiol Plant **161** : 451

Chrobok D, Law SR, Brouwer B, Linden P, Ziolkowska A, Liebsch D, Narsai R, Szal B, Moritz T, Rouhier N, Whelan J, Gardestrom P, Keech O(2016) Dissecting the metabolic role of mitochondria during developmental leaf senescence. Plant Physiol **172** : 2132–2153

Cross JM, von Korff M, Altmann T, Bartzetko L, Sulpice R, Gibon Y, Palacios N, Stitt M (2006) Variation of enzyme activities and metabolite levels in 24 Arabidopsis accessions growing in carbon-limited conditions. Plant Physiol **142:** 1574–1588

Dhatt BK, Abshire N, Paul P, Hasanthika K, Sandhu J, Zhang Q, Obata T, Walia H (2019) Metabolic Dynamics of Developing Rice Seeds Under High Night-Time Temperature Stress. Front Plant Sci. **10:**1443

Fernie AR, Roscher A, Ratcliffe RG, Kruger NJ (2001) Fructose 2,6-bisphosphate activates pyrophosphate: fructose-6-phosphate 1-phosphotransferase and increases triose phosphate to hexose phosphate cycling in heterotrophic cells. Planta **212** : 250-63

Gaufichon L, Reisdorf-Cren M, Rothstein SJ, Chardon F, SuzukiA (2010) Biological functions of asparagine synthetase in plants . Plant Sci. **179** : 141 – 153

Gaufichon L, Rothstein SJ, Suzuki A (2016) Asparagine metabolic pathways in Arabidopsis. Plant Cell Physiol. 57: 675–689.

Gibon Y, Blaesing OE, Hannemann J, Carillo P, Hohne M, Hendriks JH, Palacios N, Cross J, Selbig J, Stitt MA (2006). Robot-based platform to measure multiple enzyme activities in arabidopsis using a set of cycling assays: comparison of changes of enzyme activities and transcript levels during diurnal cycles and in prolonged darkness. Plant Cell **16:** 3304-3325

Gomez FM, Carrion CA, Costa ML, Desel C, Kieselbach T, Funk C, Krupinska K, Guiamet J (2019) Extra-plastidial degradation of chlorophyll and photosystem I in tobacco leaves involving 'senescence-associated vacuoles'. The Plant Journal **99** : 465–477

Have M, Luo J, Tellier F, Balliau T, Cueff G, Chardon F, Zivy M, Rajjou L, Cacas JL, Masclaux-Daubresse C (2019) Proteomic and lipidomic analyses of the Arabidopsis atg5 autophagy mutant reveal major changes in endoplasmic reticulum and peroxisome metabolisms and in lipid composition. New Phytologist **223** : 1461–1477.

Hildebrandt TM, Nunes Nesi A, Araujo WL, Braun HP (2015) Amino acid catabolism in plants. Mol Plant **8** : 1563–1579

Hirota T, Izumi M, Wada S, Makino A, Ishida H (2018) Vacuolar protein degradation via autophagy provides substrates to amino acid catabolic pathways as an adaptive response to sugar starvation in Arabidopsis thaliana. Plant & Cell Physiology **59** : 1363–1376

Hortensteiner S, Krautler B (2011) Chlorophyll breakdown in higher plants. Biochim Biophys Acta. **1807** : 977-988

Ishida H, Yoshimoto K, Izumi M, Reisen D, Yan Y, Makino A, Ohsumi Y, Hanson MR, Mae T (2008) Mobilization of rubisco and stroma-localized fluorescent proteins of chloroplasts to the vacuole by an ATG gene-dependent autophagic process. Plant Physiol **148:**142–155

Ishizaki K, Larson TR, Schauer N, Fernie AR, Graham IA, Leaver CJ (2005) The critical role of Arabidopsis electron-transfer flavoprotein: Ubiquinone oxido reductase during dark-induced starvation. The Plant Cell **17:** 2587-2600

Ishizaki K, Schauer N, Larson TR, Graham IA, Fernie AR, Leaver CJ (2006) The mitochondrial electron transfer flavoprotein complex is essential for survival of Arabidopsis in extended darkness. The Plant Journal **47:** 751-760

Izumi M, Hidema J, Makino A, Ishida H (2013) Autophagy contributes to nighttime energy availability for growth in Arabidopsis. Plant Physiology **161** : 1682–1693.

Izumi M, Ishida H, Nakamura S, Hidema J (2017) Entire photodamaged chloroplasts are transported to the central vacuole by Autophagy. Plant Cell **29** : 377–394

Izumi M, Nakamura S (2018) Chloroplast protein turnover: the influence of extraplastidic processes, including autophagy. Int. J. Mol. Sci . **19** : 828

Izumi M, Nakamura S, Li N (2019) Autophagic turnover of chloroplasts: its roles and regulatory mechanisms in response to sugar starvation. Frontiers in Plant Science **10** : 280.

Johnson MP, Wientjes E (2019) The relevance of dynamic thylakoid organisation to photosynthetic regulation. Biochim Biophys Acta. **1861:** 14803 doi: 10.1016/j.bbabio.2019.06.011

Kacprzak SM & van Aken O (2022) Carbon starvation, senescence and specific mitochondrial stresses, but not nitrogen starvation and general stresses, are major triggers for mitophagy in Arabidopsis. Autophagy **18** : 2894–2912

Kamranfar I, Xue GP, Tohge T, Sedaghatmehr M, Fernie AR, Balazadeh S, Mueller-Roeber, B (2018). Transcription factor RD 26 is a key regulator of metabolic reprogramming during dark-induced senescence. New Phytologist **218** :1543-1557

Kato Y, Sakamoto W (2009) Protein quality control in chloroplasts: a current model of D1 protein degradation in the photosystem II repair cycle. Journal of Biochemistry **146** : 463–469.

Lee TA, Vande-Wetering SW, Brusslan JA (2013) Stromal protein degradation is incomplete in Arabidopsis thaliana autophagy mutants undergoing natural senescence. BMC Research Notes **6** : 17–17

Li F, Chung T, Vierstra RD (2014) AUTOPHAGY-RELATED11 plays a critical role in general autophagy and senescence-induced mitophagy in Arabidopsis. Plant Cell **26** : 788–807.

Lisec J, Schauer N, Kopka J, Willmitzer L, Fernie AR (2006) Gas chromatography mass spectrometry-based metabolite profiling in plants. Nat Protoc **1** : 387–396

Livak KJ, Schmittgen TD (2001) Analysis of relative gene expression data using real-time quantitative PCR and the 2(-ΔΔC(T)) method. Methods **25** : 402–408.

Ma J, Liang Z, Zhao J, Wang P, Ma W, Mai KK, Fernandez Andrade JA, Zeng Y, Grujic N, Jiang L, Dagdas Y, Kang BH (2021) Friendly mediates membrane depolarization-induced mitophagy in Arabidopsis. Current Biology **31** (9): 1931-1944.e4.

Magen S, Seybold H, Laloum D, Avin-Wittenberg T (2022) Metabolism and autophagy in plants—a perfect match. FEBS Lett**596** : 2133-2151

Martínez DE, Costa ML, Gomez FM, Otegui MS, Guiamet JJ (2008) 'Senescence-associated vacuoles' are involved in the degradation of chloroplast proteins in tobacco leaves. The Plant Journal **56:**196–206.

Masclaux-Daubresse C, Reisdorf-Cren M, Pageau K, Lelandais M, Grandjean O, Kronenberger J, Valadier MH, Feraud M, Jouglet T, Suzuki A(2006) Glutamine synthetase–glutamate synthase pathway and glutamate dehydrogenase play distinct roles in the sink–source nitrogen cycle in tobacco. Plant Physiology **140** : 444–456.

Mazur R, Mostowska A, Szach J, Gieczewska K, Wójtowicz J, Bednarska K ., et al. (2019). Galactolipid deficiency disturbs spatial arrangement of the thylakoid network in Arabidopsis thaliana plants. J. Exp. Bot. **70** : 4689–4704.

McLoughlin F, Marshall RS, Ding X, Chatt EC, Kirkpatrick LD, Augustine RC, Li F, Otegui MS, Vierstra RD (2020) Autophagy Plays Prominent Roles in Amino Acid, Nucleotide, and Carbohydrate Metabolism During Fixed-carbon Starvation in Maize. Plant Cell. **32** : 2699–2724

Michaeli S, Galili G, Genschik P, Fernie AR, Avin-Wittenberg T(2016) Autophagy in plants: what's new on the menu? Trends Plant Sci**21** : 134–144

Michaeli S, Honig A, Levanony H, Peled-Zehavi H, Galili G(2014) Arabidopsis ATG8-INTERACTING PROTEIN1 is involved in autophagy-dependent vesicular trafficking of plastid proteins to the vacuole. Plant Cell **26** : 4084–4101

Minina EA, Moschou PN, Vetukuri RR, Sanchez-Vera V, Cardoso C, Liu Q, Elander PH, Dalman K, Beganovic M, Yilmaz JL, Marmon S, Shabala L, Suarez MF, Ljung K, Novák O, Shabala S, Stymne S, Hofius D, Bozhkov PV (2018) Transcriptional stimulation of rate-limiting components of the autophagic pathway improves plant fitness. J Exp Bot **69** : 1415–1432.

Nunes-Nesi A, Carrari F, Gibon Y, Sulpice R, Lytovchenko A, Fisahn J, Graham J, Ratcliffe RG, Sweetlove LJ, Fernie AR (2007) Deficiency of mitochondrial fumarase activity in tomato plants impairs photosynthesis via an effect on stomatal function. Plant J **50** : 1093–1106.

Oh SA, Lee SY, Chung IK, Lee CH, Nam HG (1996) A senescence-associated gene of Arabidopsis thaliana is distinctively regulated during natural and artificially induced leaf senescence. Plant Mol Biol **30** : 739–754

Otegui MS, Noh YS, Martı´nez DE, Vila Petroff MG, Staehelin LA, Amasino RM, Guiamet JJ (2005) Senescence-associated vacuoles with intense proteolytic activity develop in leaves of Arabidopsis and soybean. Plant J **41** : 831–844

Otegui MS (2017) Vacuolar degradation of chloroplast components: autophagy and beyond. J. Exp. Bot. **69** : 741–750

Peleg Z, Reguera M, Tumimbang E, Walia H, Blumwald E (2011) Cytokinin-mediated source/sink modifications improve drought tolerance and increase grain yield in rice under water-stress. Plant Biotechnology Journal **9** : 747–758.

Porra RJ, Thompson WA, Kriedemann PE (1989) Determination of accurate extinction coefficients and simultaneous equations for assaying chlorophylls a and b extracted with four different solvents: verification of the concentration of chlorophyll standards by atomic absorption spectroscopy. Biochim Biophys Acta **975** : 384–394

Sade N, Umnajkitikorn K, Rubio Wilhelmi M, Wright M, Wang S, Blumwald E (2018) Delaying chloroplast turnover increases water-deficit stress tolerance through the enhancement of nitrogen assimilation in rice. J. Exp. Bot. **69:** 867–878

Shibata M, Oikawa K, Yoshimoto K, Kondo M, Mano S, Yamada K, Hayashi M, Sakamoto W, Ohsumi Y, Nishimura M (2013) Highly oxidized peroxisomes are selectively degraded via autophagy in Arabidopsis. Plant Cell **25** : 4967–4983.

Thompson AR, Doelling JH, Suttangkakul A, Vierstra RD (2005) Autophagic nutrient recycling in Arabidopsis directed by the ATG8 and ATG12 conjugation pathways. Plant Physiol **138** : 2097–2110

Umnajkitikorn K, Sade N, Wilhelmi MDMR, Gilbert ME, Blumwald E(2020) Silencing of OsCV (chloroplast vesiculation) maintained photorespiration and N assimilation in rice plants grown under elevated CO2. Plant Cell Environ. **43:** 920–933

Wada S, Ishida H, Izumi M, Yoshimoto K, Ohsumi Y, Mae T, Makino A (2009) Autophagy plays a role in chloroplast degradation during senescence in individually darkened leaves. Plant Physiology**49** : 885–893

Wang S, Blumwald E (2014) Stress-induced chloroplast degradation in Arabidopsis is regulated via a process independent of autophagy and senescence-associated vacuoles. Plant Cell **26:**4875–488

Watanabe M, Balazadeh S, Tohge T, Erban A, Giavalisco P, Kopka J, Mueller-Roeber B, Fernie AR, Hoefgen R (2013) Comprehensive dissection of spatio-temporal metabolic shifts in primary, secondary and lipid metabolism during developmental senescence in Arabidopsis thaliana. Plant physiology **162:** 1290-1310

Woodson JD (2022) Control of chloroplast degradation and cell death in response to stress. Trends Biochem Sci.**47** (10):851-864. doi: 10.1016/j.tibs.2022.03.010.

Xie Q, Michaeli S, Peled-Zehavi H, Galili G (2015) Chloroplast degradation: One organelle, multiple degradation pathways. Trends in Plant Science **20** : 264–265

Yu JC, Lu JZ, Cui XY, Guo L, Wang ZJ, Liu YD, Li TL (2022) Melatonin mediates reactive oxygen species homeostasis via SlCV to regulate leaf senescence in tomato plants. J. Pineal Res. 73. 10.1111/jpi.12810.

Yoshimoto K, Shibata M, Kondo M, Oikawa K, Sato M, Toyooka K, Shirasu K, Nishimura M, Ohsumi Y (2014) Organ-specific quality control of plant peroxisomes is mediated by autophagy. J Cell Sci **127** : 1161–1168

FIGURES

Figure 1

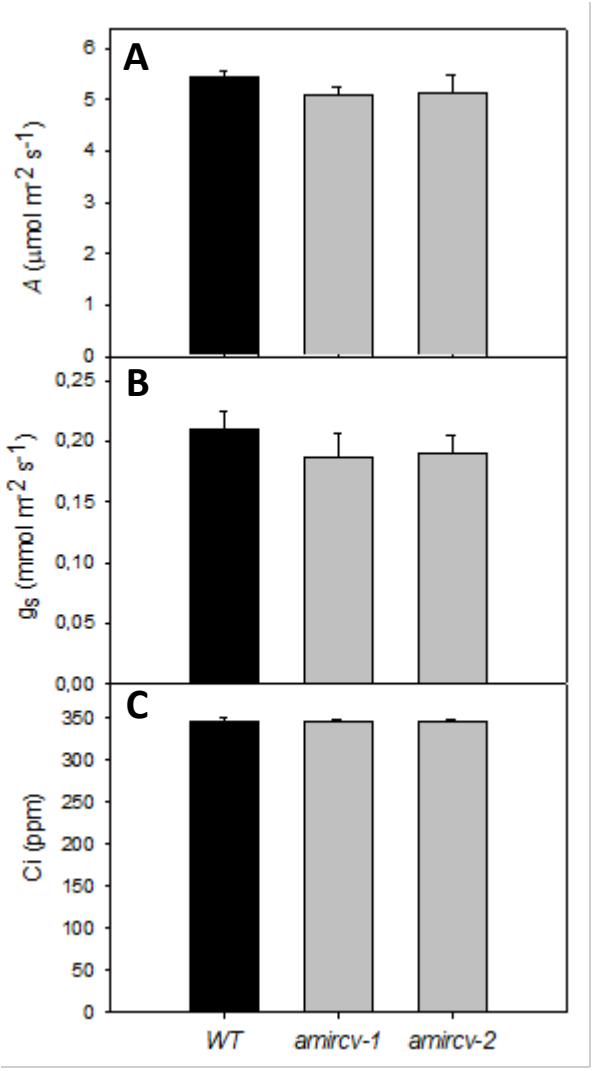

Figure 1. Gas-exchange parameters are not affected in wild-type (WT) and *amircv* mutants.

(A) net CO_2 assimilation rate (A), (B) stomatal conductance (g_s), (C) internal CO_2 concentration (C_i). Values presented are means ± SE of five biological replicates per genotype. No significant differences were determined by the Student's t test ($P < 0.05$) between WT and mutant lines in each time point analyzed.

Figure 2

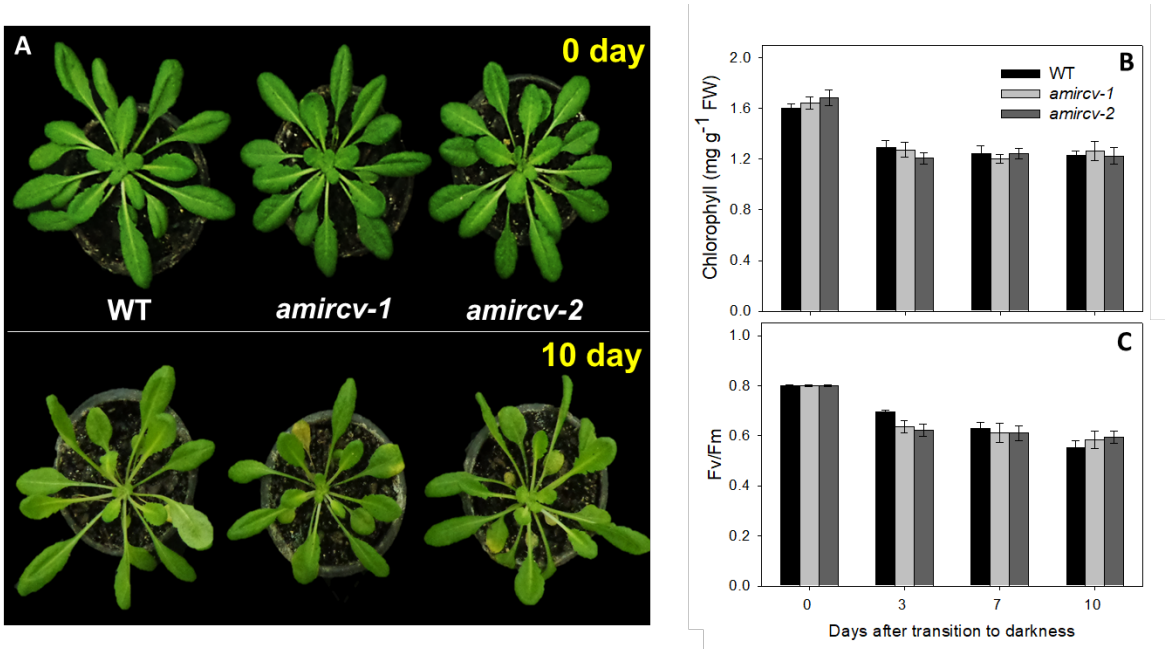

Figure 2. Phenotype of *amircv* Arabidopsis mutants under extended darkness

(A) Images of 4-week-old, short-day-grown Arabidopsis plants immediately (0 day) and after treatment for 10 days in darkness conditions; (B) Chlorophyll content; (C); Fv/Fm, the maximum quantum yield of PSII of leaves of 4-week-old plants after further treatment for 0, 3, 7 and 10 d in darkness. Values are means ± SE of five independent samplings; no significant differences were determined by the Student's t test ($P < 0.05$) between wild-type (WT) and mutant lines in each time point analyzed; FW, fresh weight.

Figure 3

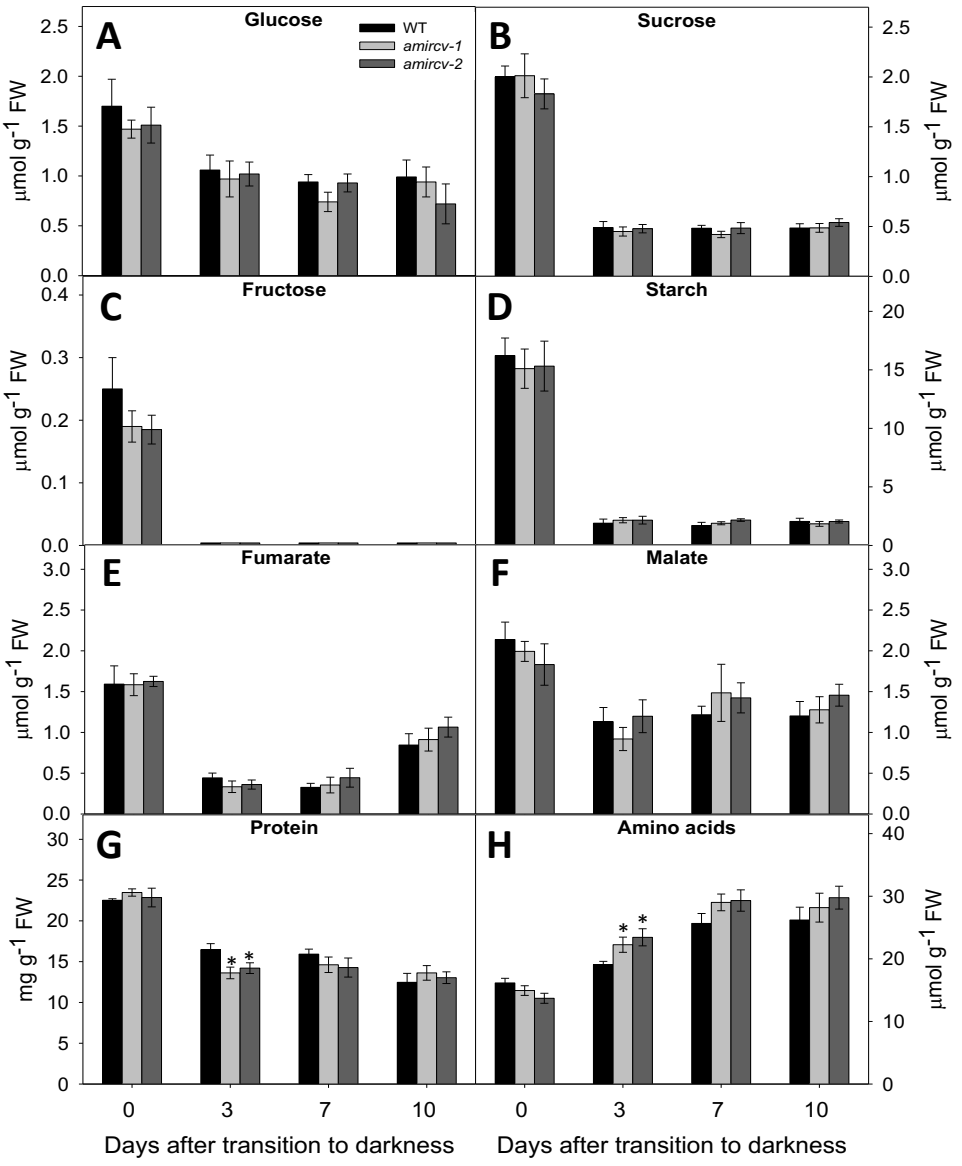

Figure 3. Metabolite levels in *amircv Arabidopsis* mutants under extended darkness. (A) Glucose, (B) sucrose, (C) fructose, (D) starch, (E) fumarate, (F) malate, (G) total protein and (H) total free amino acids. Values presented are means ± SE of five biological replicates per genotype; an asterisk (*) designate values that were determined by the Student's *t*-test to be significantly different ($P < 0.05$) from the wild-type (WT).

Figure 4

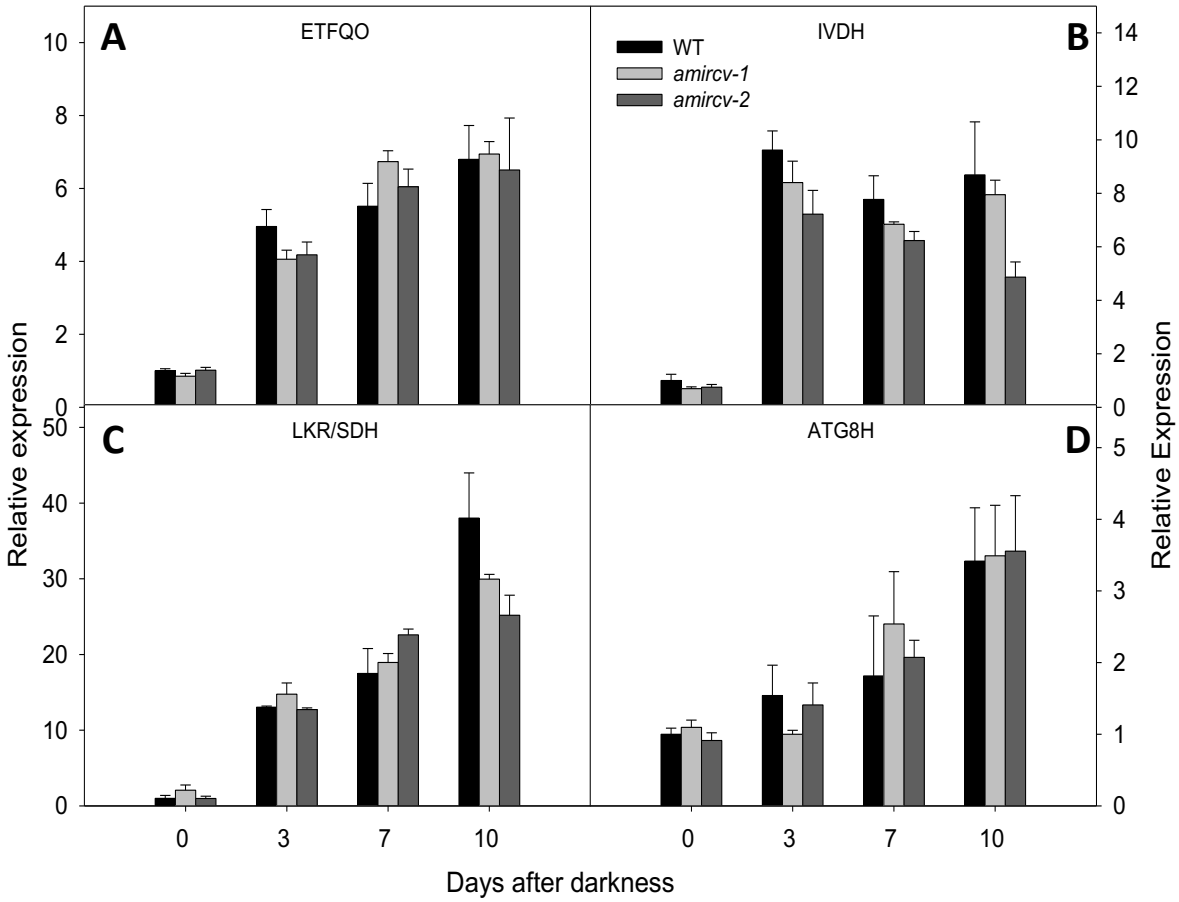

Figure 4. Transcript levels of genes related to alternative pathways of respiration and autophagy in *amircv* Arabidopsis mutants.

(A) Electron transfer flavoprotein/ ubiquinone oxireductase ETFQO; (B) Isovaleryl-CoA dehydrogenase- IVDH; (C) Lysine-ketoglutarate reductase/sacharopine dehydrogenase- LKR/SDH (D) Autophagy gene -ATG8h. The y-axis values represent the expression level relative to the wild-type (WT). Data were normalized with respect to the mean response calculated for the 0-d dark-treated leaves of the WT. Values presented are means ± SE of at least three independent biological replicates.

Figure 5

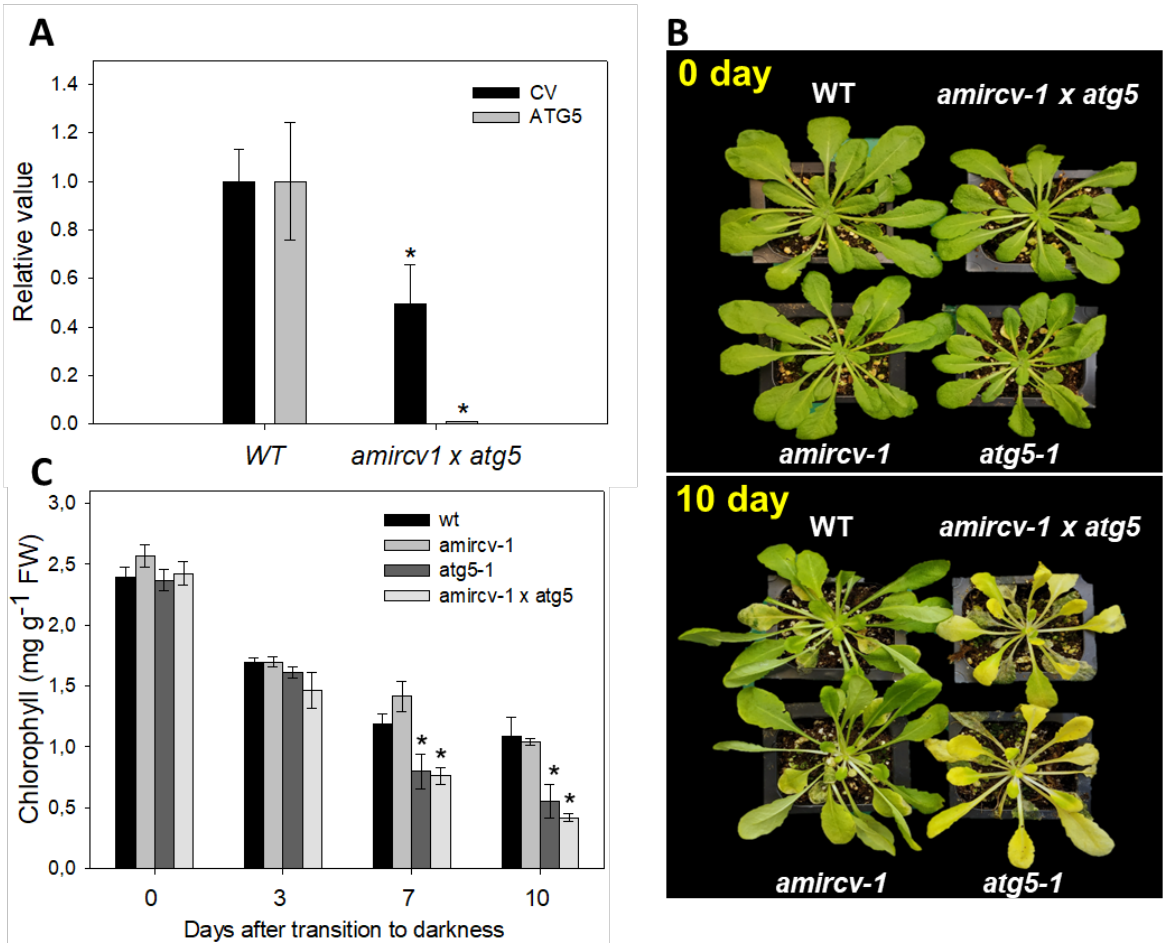

Figure 5. Phenotype of Arabidopsis *amircv1xatg5* mutants under extended darkness.

(A) Confirmation of low expression of *CV* and *ATG5* genes by RT-qPCR *amircv1xatg5* plants. Values are means ± SE of three biological replicates. An asterisk (*) designate expression values that were determined by the Student's t-test to be significantly different ($P < 0.05$) from wild-type (WT) for each gene analyzed (B) Representative images of 4-week-old, short-day-grown Arabidopsis plants immediately (0 d) and after further treatment for 10 days in darkness conditions. (C) Chlorophyll content of leaves of 4-week-old, short-day-grown. Values presented are means ± SE of five biological replicates. an asterisk (*) designate values that were determined by the Student's t-test to be significantly different ($P < 0.05$) from WT each time point. FW, fresh weight.

Figure 6

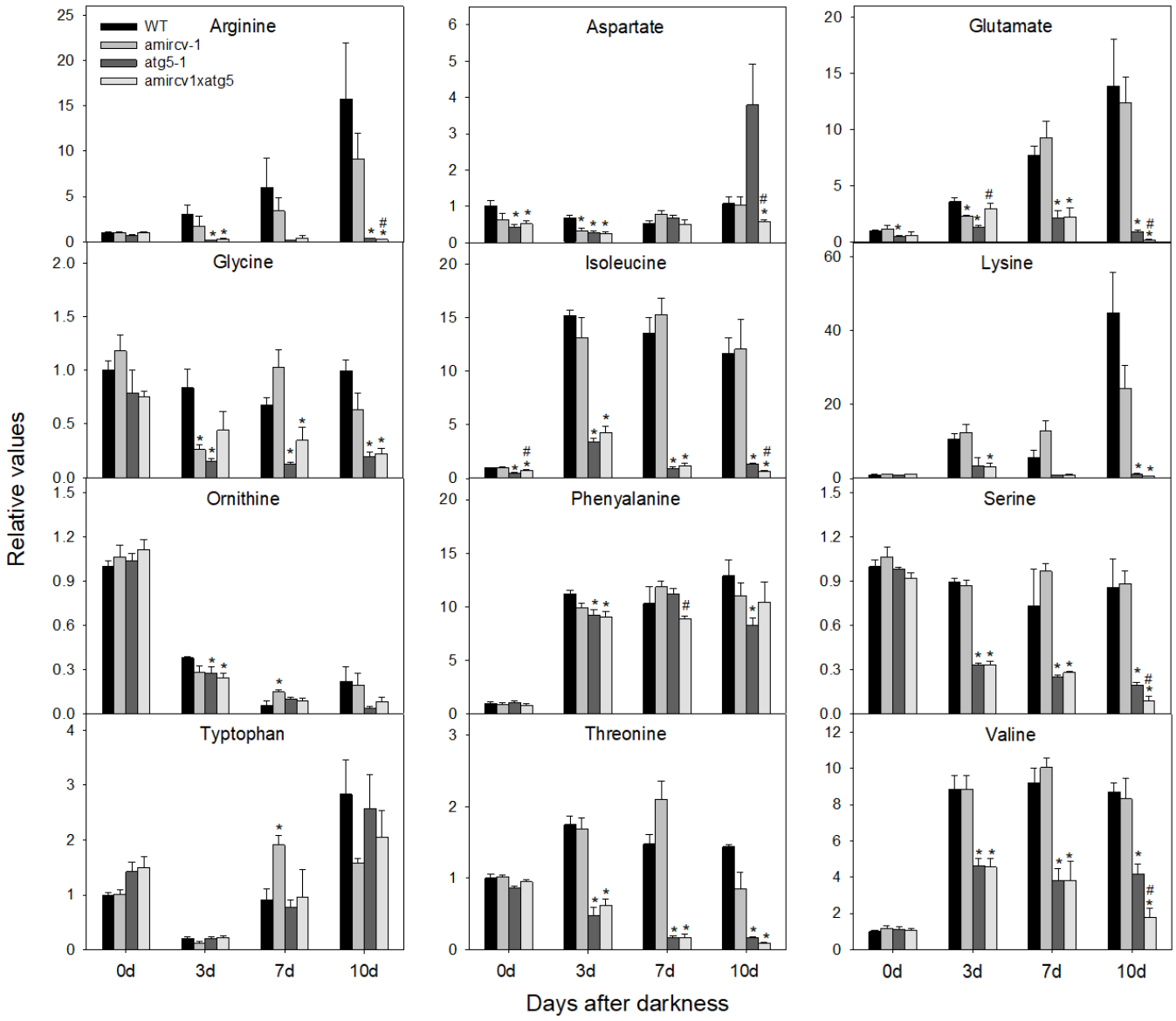

Figure 6. Effects of both CV and autophagy mutation on amino acids levels during extended darkness conditions.

Metabolite profile of Arabidopsis *amircv1xatg5* , *atg5, amircv-1* and wild-type (WT) genotypes during extended dark conditions. Data were normalized to the mean response calculated for the 0-d dark treated leaves of the WT. Values presented are means ± SE of four biological replicates per genotype; an asterisk (*) designate values that were determined by the Student's t-test to be significantly different ($P < 0.05$) from WT each time point. The hash (#) designate *amircv1xatg5* values that were determined by the Student's *t*-test to be significantly different ($P < 0.05$) from *atg5* each time point.

Figure 7

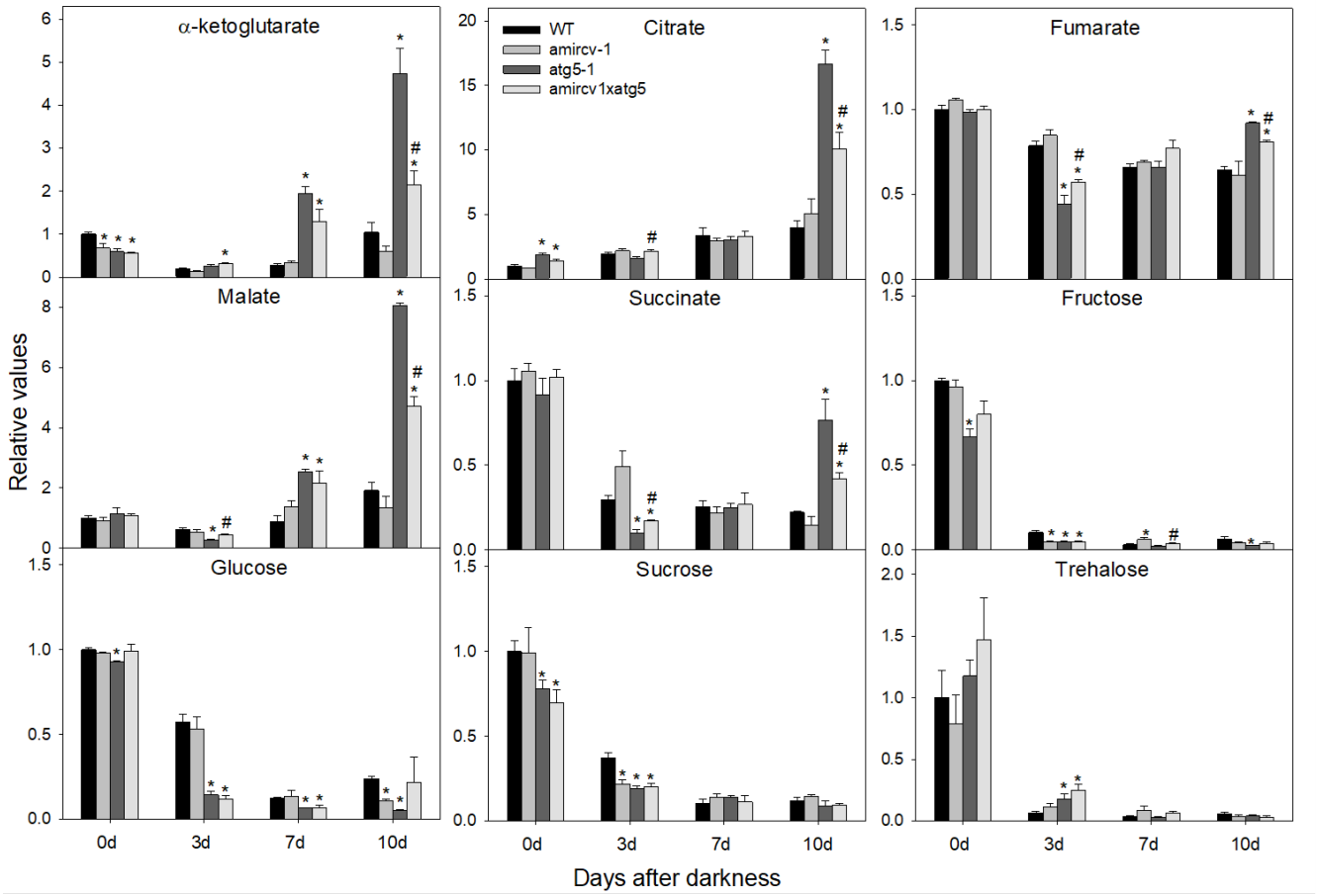

Figure 7. Effects of both CV and autophagy mutation on organic acids levels during extended darkness conditions.

Metabolite profile of Arabidopsis *amircv1xatg5 atg5, amircv-1* and wild-type (WT) genotypes during extended dark conditions. Data were normalized to the mean response calculated for the 0-d dark treated leaves of the WT. Values presented are means ± SE of four biological replicates per genotype; an asterisk (*) designate values that were determined by the Student's t-test to be significantly different ($P < 0.05$) from WT each time point. The hash (#) designate *amircv1xatg5* values that were determined by the Student's *t*-test to be significantly different ($P < 0.05$) from *atg5* each time point.

Figure 8

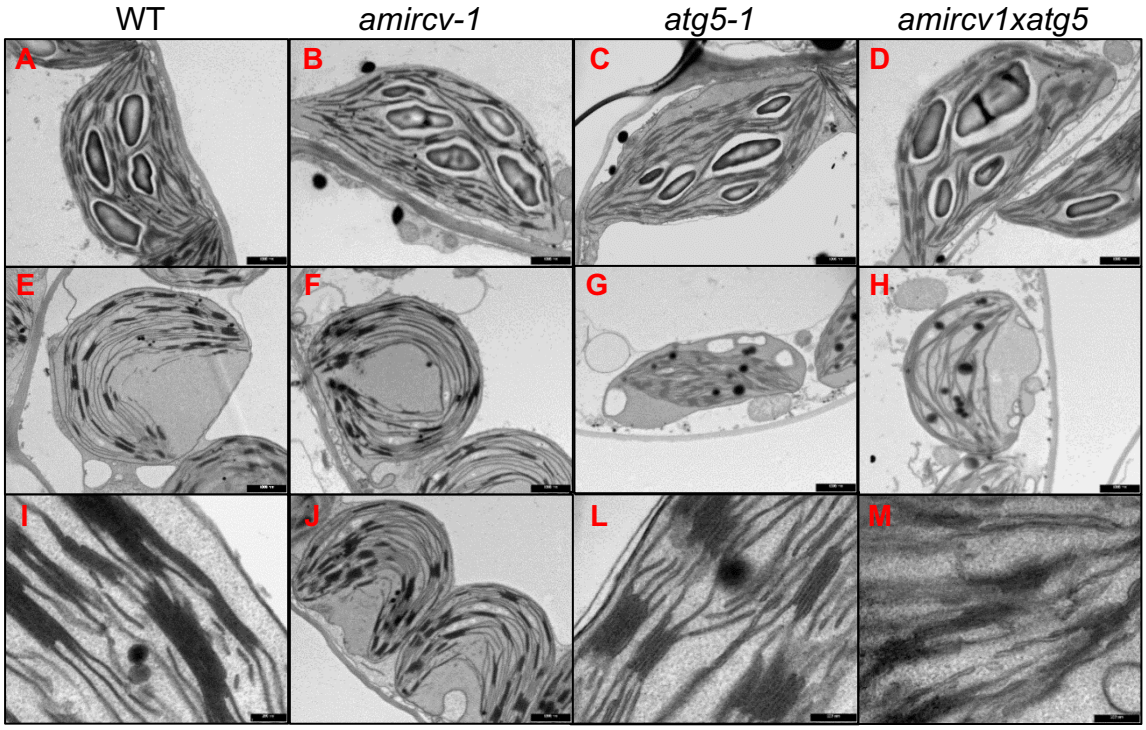

Figure 8. Abnormal chloroplast accumulation of *atg5-1* and *amicv1 x atg5* mutants.

Transmission electron micrographs of leaves of wild-type (WT), *amircv-1*, *atg5-1* and *amir1xatg5* plants immediately (0d) and after7 days of darkness (E-M). Scale bar = 1 µm in images A-H and J; Scale bar = 0.2 µm in images I,L,M.